

Polymers and oligomers derived from pyrrole and *N*-hydroxymethylpyrrole: A theoretical analysis of the structural and electronic properties

Cintia Ocampo^a, Jordi Casanovas^{b,*}, Francisco Liesa^c, Carlos Alemán^{a,*}

^a *Departament d'Enginyeria Química, ETSEIB, Universitat Politècnica de Catalunya, Diagonal 647, Barcelona E-08028, Spain*

^b *Departament de Química, Escola Politècnica Superior, Universitat de Lleida, c/Jaume II n° 69, Lleida E-25001, Spain*

^c *Departament d'Enginyeria Mecànica, ETSEIB, Universitat Politècnica de Catalunya, Diagonal 647, Barcelona E-08028, Spain*

Received 28 October 2005; received in revised form 20 February 2006; accepted 21 February 2006

Available online 23 March 2006

Abstract

This work reports a theoretical investigation about the structural and electronic properties of polymers constituted by pyrrole and *N*-hydroxymethylpyrrole in both neutral and p-doped states. Ab initio quantum mechanical calculations were performed on neutral and positively charged oligomers to evaluate the bond length alternation pattern in the π -system, the molecular conformation, the π - π^* transition energies and the ionization potential. Results, which have been extrapolated to infinite polymer chains, allow analyze the influence of *N*-hydroxyalkylation of polypyrrole on these properties.

© 2006 Elsevier Ltd. All rights reserved.

Keywords: Polypyrrole; *N*-Hydroxyalkylation; Quantum mechanics

1. Introduction

A crucial step in the continuing effort to develop new conjugated polymers has been the addition of substituents on the monomer. Thus, the introduction of substituents has been used not only to induce changes in the structure and electronic properties but also to confer solubility and improve the process ability of these materials. In this context, quantum mechanical calculations on small oligomers have been extensively and successfully used to predict the substitutional effects [1–5].

Early studies indicated that the electrical conductivity of materials obtained by alkylating the nitrogen atom of pyrrole is worse than that of the unsubstituted polypyrrole [6,7], while alkylation on the β -carbon atom can produce polymers with better conductivity if prepared under optimized conditions [8]. On the other hand, the molecular and electronic structure of some alkyl-substituted 2,2'-bipyrroles were investigated, using quantum mechanical techniques, to provide an improved understanding of these materials [5,9].

In a very recent study [10], we used theoretical methods to analyze the effects produced by hydroxyalkyl substitution on the *N*-position of the pyrrole ring. Thus, calculations based on the density functional theory (DFT) were used to ascertain the structural properties of 2,2'-bipyrroles *N*-substituted with hydroxymethyl and hydroxypropyl (2-MeOHPy and 2-PrOHPy, respectively) in a neutral state. Furthermore, the band gap (ϵ_g) of the 2-MeOHPy was predicted to be smaller than that of 2,2'-bipyrrole (2-Py) when a planar anti conformation is considered.

In this work, we extend our studies about the effects produced by *N*-hydroxyalkyl substitution on the properties of pyrrole-containing oligomers considering both larger oligomers and the p-doped state. For this purpose, molecular chains formed by *n* rings of *N*-hydroxymethylpyrrole and pyrrole (*n*-MeOHPy and *n*-Py, respectively) have been calculated in both the neutral and positively charged states.

2. Methods

All the calculations were performed using the Gaussian 98 program [11]. The structures of neutral (*n*-MeOHPy and *n*-Py) oligomers were fully optimized in the gas-phase at the Hartree–Fock (HF) level using as starting point the all-anti conformation, i.e. the inter-ring dihedral angles N–C–C–N (θ_i , where *i* ranges from 1 to *n*–1) arranged at 180°. The molecular geometries of *n*-MeOHPy⁺² and *n*-Py⁺² oligomers were

* Corresponding authors.

E-mail addresses: jcasanovas@quimica.udl.es (J. Casanovas), carlos.aleman@upc.es (C. Alemán).

optimized without any constraint at the unrestricted Hartree–Fock (UHF) level using as starting points the fully optimized structures of the corresponding neutral oligomers. The hydroxyl groups of *n*-MeOHPy and *n*-MeOHPy⁺² were initially arranged considering the most favored orientation detected for 2-MeOHPy in our previous study [10]. Additionally, constrained geometry optimizations, in which all the inter-ring dihedral angles were fixed at 180°, were performed for neutral oligomers. The number of rings *n* considered in neutral oligomers ranged from 1 to 8 and 16 for *n*-MeOHPy and *n*-Py, respectively, while the largest value of *n* for *n*-MeOHPy⁺² and *n*-Py⁺² was 6 and 12, respectively. The 6-31G(d) basis set [12], which can be described as a valence double zeta basis with a set of polarizing d-functions on the non-hydrogen atoms, was used in all the calculations. Calculations performed using HF and UHF methods combined with the 6-31G(d) basis set will be denoted HF/6-31G(d) and UHF/6-31G(d), respectively.

The benzoid and quinoid structures of the optimized oligomers were examined using two parameters: δ_{inter} and δ_{ring} . These bond alternation parameters were calculated according to

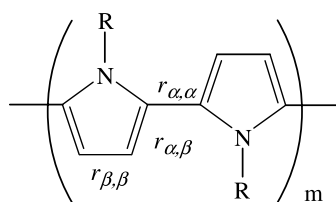
$$\delta_{\text{inter}} = \frac{r_{\alpha,\alpha} - r_{\alpha,\beta}}{(r_{\alpha,\alpha} + r_{\alpha,\beta})/2} \quad (1)$$

$$\delta_{\text{ring}} = \frac{r_{\beta,\beta} - r_{\alpha,\beta}}{(r_{\beta,\beta} + r_{\alpha,\beta})/2} \quad (2)$$

where $r_{\alpha,\alpha}$ denotes the inter-ring bond length, and $r_{\alpha,\beta}$ and $r_{\beta,\beta}$ are the intra-ring bond lengths as labeled in Scheme 1.

The Koopmans' theorem [13] was used to estimate the ionization potentials (IPs). Accordingly, IPs were taken as the negative of the highest occupied molecular orbital (HOMO) energy, i.e. $\text{IP} = -\epsilon_{\text{HOMO}}$. The IP indicates if a given acceptor (p-type dopant) is capable of ionizing, at least partially, the molecules of the compound. The π - π^* transition energies (ϵ_g), which corresponds to the gap, were approximated as the difference between the HOMO and lowest unoccupied molecular orbital (LUMO) energies, i.e. $\epsilon_g = \epsilon_{\text{LUMO}} - \epsilon_{\text{HOMO}}$.

We are aware that HF calculations overestimate the values of ϵ_g . However, it should be emphasized that this method provides a satisfactory qualitative description of the electronic properties of polyheterocyclic molecules like those studied in this work [5,14]. Accordingly, the ϵ_g and IP values presented in this work should be considered in relative terms.



n-Py: R=H, *n*=*m*-2

n-MeOHPy: R=CH₂OH, *n*=*m*-2

Scheme 1. Systems investigated in this work.

To estimate the free energies of solvation (ΔG_{sol}) of *n*-Py and *n*-MeOHPy oligomers, calculations were performed using the polarizable continuum model (PCM) [15]. This is a self-consistent reaction-field (SCRF) model that treats the solute at the quantum mechanical level, while the solvent is represented as a dielectric continuum. More specifically, the PCM method involves the generation of a solvent cavity from spheres centered at each atom in the molecule and the calculation of virtual point charges on the cavity surface representing the polarization of the solvent. The magnitude of these charges is proportional to the derivative of the solute electrostatic potential at each point calculated from the molecular wave function. Thus, point charges may, then, be included in the one-electron Hamiltonian, thus inducing polarization of the solute. An iterative calculation is carried out until the wave function and the surface charges are self consistent. PCM calculations were performed at the HF/6-31G(d) level using the dielectric constant of water ($\epsilon=78.4$). It should be emphasized that previous studies indicated that solute geometry relaxations in solution and single point calculations using the solute geometries optimized in the gas-phase produce almost identical ΔG_{sol} values [16–18]. Accordingly, all the PCM calculations presented in this work were carried out using the structures optimized in the gas-phase.

3. Results and discussion

3.1. Effects of *N*-hydroxyalkylation on neutral compounds

3.1.1. Geometry

Table 1 shows the average of the more relevant geometric parameters calculated for *n*-Py and *n*-MeOHPy. Complete geometry optimizations of *n*-Py with *n* ranging from 1 to 16 provided an anti-gauche conformation, i.e. $|\theta| \approx 150^\circ$, which is in excellent agreement with results previously obtained for 2-Py using HF, DFT, second-order Møller–Plesset perturbation theory (MP2) and fourth-order Møller–Plesset perturbation theory (MP4) methods [5,9,10,19,20]. In contrast, geometry optimizations of *n*-MeOHPy with *n* ranging from 1 to 8 led to a gauche–gauche conformation, i.e. $|\theta| \approx 80^\circ$. Obviously, the reason of these drastic conformational differences has to be found in the repulsive steric interactions generated by the hydroxymethyl substituents. These unfavorable interactions are also responsible of differences in the inter-ring bond distances $r_{\alpha,\alpha}$, which are larger for *n*-MeOHPy than for *n*-Py by ~ 0.01 Å. Consistently, the average inter-ring alternation

Table 1
Optimized geometries of *n*-Py (*n*=1–16) and *n*-MeOHPy (*n*=1–8)

Compounds	$ \theta ^a$	$r_{\alpha,\alpha}^b$	δ_{inter}^c	δ_{ring}^d
<i>n</i> -Py	150.3	1.465	0.072	0.041
<i>n</i> -MeOHPy	80.5	1.473	0.080	0.045

^a Average inter-ring dihedral angle N–C–C–N (in degrees).

^b $r_{\alpha,\alpha}$ is the average inter-ring bond distance (in Å).

^c δ_{inter} is the average inter-ring bond alternation parameter (in Å). See Eq. (1).

^d δ_{ring} is the average intra-ring bond alternation parameter (in Å). See Eq. (2).

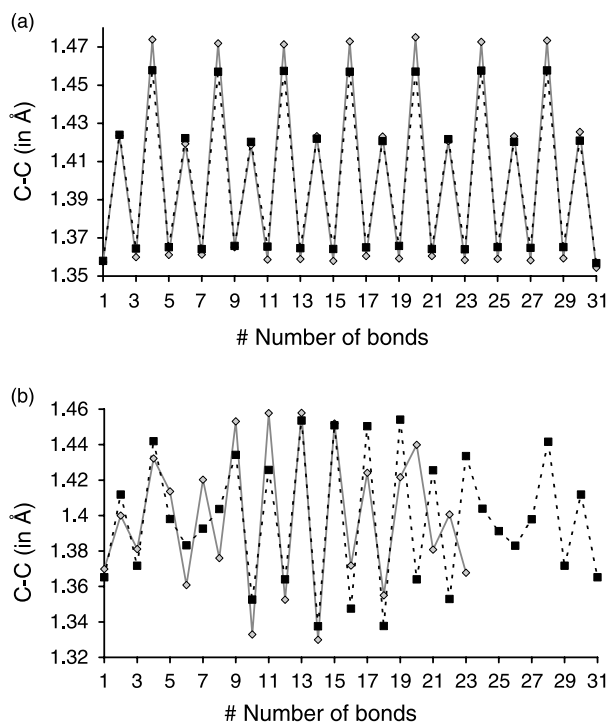


Fig. 1. Behavior of the C–C bond length along the conjugated π -system of (a) neutral 8-Py (black squares connected by dotted lines) and 8-MeOHPy (gray diamonds connected by solid lines); and (b) charged 8-Py⁺² (black squares connected by dotted lines) and 6-MeOHPy⁺² (gray diamonds connected by solid lines).

parameter, δ_{inter} , is 0.008 Å higher for the former compounds. However, difference in the intra-ring bond alternation parameters, δ_{ring} , decreases to 0.004 Å indicating that the *N*-substitution effects are more important for the π -conjugative effects between the rings than for the π -system within the ring.

The benzenoid structure of *n*-Py and *n*-MeOHPy is represented in Fig. 1(a), where the C–C bond lengths along the conjugated π -system of 8-Py and 8-MeOHPy are represented. As can be seen, the bond alternation is more marked in 8-MeOHPy. Therefore, the values obtained for the C–C and C=C bond lengths are fully consistent with the conclusions reached from the comparison between the inter- and intra-ring alternation parameters. It should be mentioned that patterns of neutral oligomers with $n \neq 8$ do not provide any additional finding. The benzenoid structure characteristic of neutral compounds is lost upon oxidation as reflects the bond length alternation pattern predicted for dicationic compounds (see below), which is displayed in Fig. 1(b).

3.1.2. Electronic properties

Fig. 2 represents the variation of ϵ_g and IP with inverse chain length ($1/n$) for *n*-Py and *n*-MeOHPy calculated using the fully optimized geometries. The representation of electronic properties against $1/n$ has been demonstrated to provide satisfactory results for infinite polymer chains by simple regression analysis [21,22]. For $n > 2$ the ϵ_g predicted for *n*-MeOHPy is considerably larger than that calculated for *n*-Py. Similarly, the differences between the IP obtained for the two families of

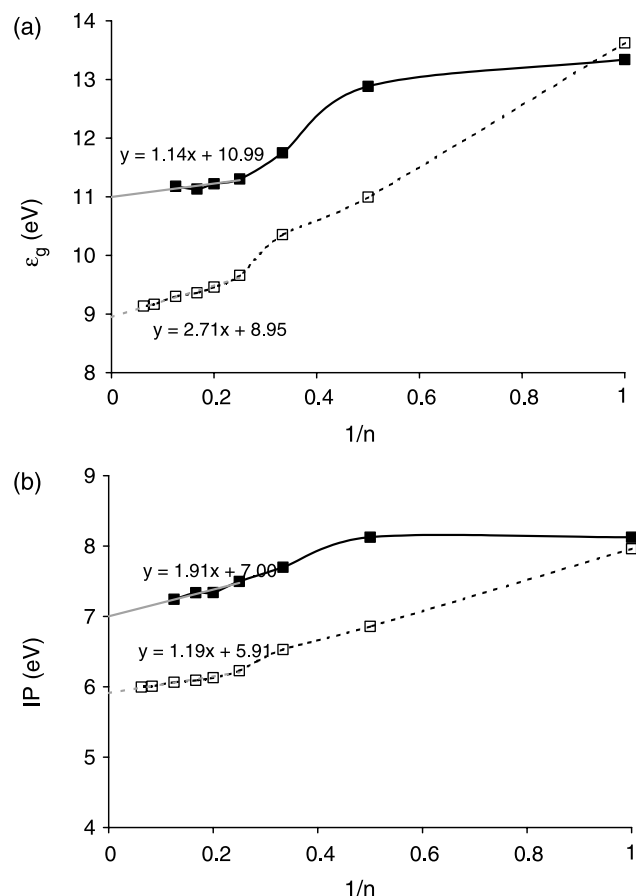


Fig. 2. Evolution of the ϵ_g (a) and IP (b) with inverse chain length ($1/n$) calculated for *n*-MeOHPy (black squares, solid lined) and *n*-Py (white squares, dashed line) using the fully optimized geometries.

oligomers increase with the number of chemical units. On the other hand, the linear behavior followed by these electronic parameters, which only appears for $n > 3$ in both systems, is quite rough. This should be attributed to the structural distortions produced by the apparition of equivalent rotamers within the same chain during geometry optimizations. For example, the inter-ring dihedral angles obtained for the minimum energy conformations of *n*-Py with $n > 3$ consist on combinations of rotamers with $\theta \approx +150^\circ$ and -150° rather than on repetitions of a single rotamer $\theta \approx +150^\circ$. The same behavior is observed for *n*-MeOHPy but with the inter-ring dihedral angles $\theta \approx +80^\circ$ and -80° . Unfortunately, it was not possible to consider all the conformations produced by such equivalent rotamers since quantum mechanical calculations require a huge amount of computer resources. However, the influence of such rotamers on the energies of the HOMO and LUMO orbital was investigated by considering the compounds with $n = 3$. It was found that this conformational effect changes the orbitalic energies by 0.09 eV in average. This small value is not expected to alter the conclusions reached in the present study.

The values of ϵ_g extrapolated for an infinite chain of MeOHPy and Py, i.e. poly(MeOHPy) and poly(Py), which

were obtained through a linear regression of the data predicted for $n > 3$ (Fig. 2), are 10.99 and 8.95 eV, respectively. The same procedure was used to obtain the IPs, the resulting values being 7.00 and 5.91 eV, respectively. In all cases, the correlation coefficients (R^2) range from 0.68 to 0.96.

In order to analyze if the electronic properties of n -MeOHPy and n -Py improve with the planarity, all the structures were re-optimized but fixing the inter-ring dihedral angles at $\theta = 180^\circ$ (all-anti conformation). The variations of ε_g and IP with inverse chain length ($1/n$) calculated for the re-optimized structures are displayed in Fig. 3. A perfect linear behavior was obtained for n -Py, while n -MeOHPy shows small distortions associated to the arrangement of the methoxy groups. However, it should be noted that ε_g is smaller for n -MeOHPy oligomers than for n -Py independently of n . Using linear regressions, which are included in Fig. 3, ε_g values of 7.26 and 7.98 eV were extrapolated for poly(MeOHPy) and poly(Py), respectively. Thus, the ε_g values decreases by 34 and 11%, respectively, when the planar conformation is forced. On the other hand, inspection to the Fig. 3(b) indicates that the IP is slightly smaller for n -Py than for n -MeOHPy, the values extrapolated for an infinite chain being 5.46 and 5.60 eV, respectively. This difference, 0.14 eV, is considerably smaller than that between the ε_g values, 0.72 eV, suggesting that N -hydroxyalkyl

substitution of neutral poly(Py) mainly affects to the stability of the LUMO. Furthermore, the geometrical restrictions imposed to retain the all-anti conformation increase the HOMO energy by 20 and 8% in poly(MeOHPy) and poly(Py), respectively, with respect to the values predicted for the fully optimized conformations.

3.1.3. Relative energies and solvent effects

The interesting electronic properties predicted for the all-anti conformation of n -MeOHPy points out that the relative stability of this structure with respect to the fully optimised one should be examined in more detail. Fig. 4(a) shows the variation of the relative energy in the gas-phase between the fully optimized and all-anti conformations against n for n -Py and n -MeOHPy. As can be seen, the change from gauche-gauche to anti conformation produces a destabilization of 6–7 kcal/mol per MeOHPy unit, while the energy increases by only 0.5 kcal/mol per Py unit when the anti-gauche conformation becomes planar. The large energy penalty required by n -MeOHPy points out that the improvement of the π - π interactions between adjacent rings is achieved by imposing a very high strain to the system.

In order to investigate the influence of the aqueous solvent on the relative stability of such two conformations, the ΔG_{sol} values were computed for both n -Py and n -MeOHPy oligomers. According to the classical thermodynamical

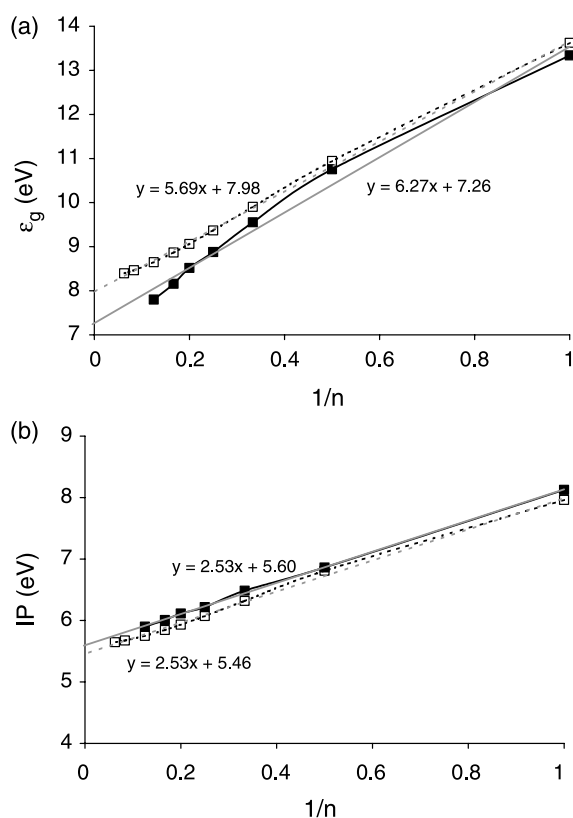


Fig. 3. Evolution of the ε_g (a) and IP (b) with inverse chain length ($1/n$) calculated for n -MeOHPy (black squares, solid line) and n -Py (white squares, dashed line) using the relaxed all-anti geometry, which was obtained by fixing the inter-ring dihedral angles (θ) at 180° and optimizing the rest of the molecular geometric parameters.

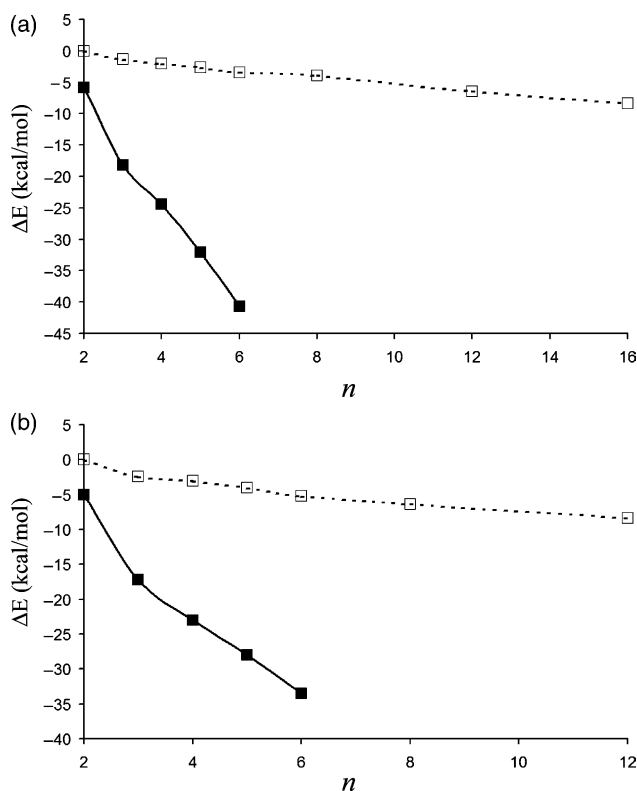


Fig. 4. Variation of the relative energy in the gas-phase (a) and aqueous solution (b) between the fully optimized and all-anti conformations against n for n -Py (white squares, dashed line) and n -MeOHPy oligomers (black squares, solid line).

scheme, total energies in aqueous solution were obtained by adding the ΔG_{sol} values to the gas-phase energies. Fig. 4(b) displays the variation of the relative energy in solution between the fully optimized and the all-anti conformation for the two families of oligomers. For *n*-MeOHPy the gauche–gauche resulted again more stable than the planar anti conformation, although the bulk solvent reduces the energy difference to ~ 5.5 kcal/mol per MeOHPy unit. Regarding to *n*-Py oligomers, the aqueous environment increased the relative energy of the planar conformation to ~ 0.7 kcal/mol per Py unit. Thus, the solvent produces an opposite effect in *n*-MeOHPy and *n*-Py oligomers, which must be attributed to the hydrophilicity of the hydroxyl group. This is reflected by the ΔG_{sol} , which indicates that the interaction of the bulk solvent with *n*-MeOHPy is more favourable than with *n*-Py for a given value of *n*. Thus, for a given *n*, the ΔG_{sol} value calculated for the *n*-Py oligomer is in average $0.8n$ kcal/mol less negative than that obtained for *n*-MeOHPy.

3.2. Effects of *N*-hydroxyalkylation on dicationic compounds

3.2.1. Geometry

The full optimization of all the *n*-Py²⁺ oligomers led to an all-anti conformation, the inter-ring dihedral angle being $|\theta| \approx 180 \pm 1^\circ$ in average. This planar arrangement is fully consistent with the quinoid structure expected for charged oligomers, which is shown in Fig. 1(b) for 8-Py²⁺. It is worth noting that the C–C bond length alternation pattern is reversed with respect to that obtained for neutral 8-Py (Fig. 1(a)). As expected, the quinoid defect is maximal at the center of the *n*-Py²⁺ oligomers and minimum at the rings near to the ends of the molecules. Thus, the quinoid defect disappears at the end rings for oligomers with $n \geq 5$. An analysis of the extension of the maximum and minimum regions of all *n*-Py²⁺ oligomers indicates that the spatial extension of the quinoid defect is about four rings for $n \geq 6$. The overall of these results is in excellent agreement with those obtained earlier using simple semiempirical methods [23].

On the other hand, energy minimizations of *n*-MeOHPy²⁺ led to an all-anti conformation with $|\theta| \approx 170 \pm 5^\circ$ in all cases. Thus, the positive doping of hydroxymethylated oligomers induce a change of about 90° in the inter-ring dihedral angles, i.e. the conformation changes from gauche–gauche to anti, which is consistent with a strong transition benzenoid \rightarrow quinoid in the electronic structure. Thus, examination of the C–C bond lengths along the conjugated π -system revealed that the double bond character of the inter-ring bonds is slightly higher for *n*-Py²⁺ than for *n*-MeOHPy²⁺. This is shown in Fig. 1(b), which shows the bond length alternation pattern of 6-MeOHPy²⁺. The averaged inter-ring C–C bond (excluding the values associated to the first and last rings) is 1.366 and 1.359 Å for 6-MeOHPy²⁺ and 6-Py²⁺, respectively. Table 2 compares the more relevant geometric parameters for such two dicationic oligomers, which were averaged taking into account only the four central rings.

It should be noted that the average deviation of the inter-ring dihedral angles with respect to the ideal planarity ($\theta = 180^\circ$) was

Table 2
Optimized geometries^a of 6-Py²⁺ and 6-MeOHPy²⁺

Compounds	$ \theta ^b$	$r_{\alpha,\alpha}^c$	δ_{inter}^d	δ_{ring}^e
6-Py ²⁺	180.0	1.359	−0.067	−0.077
6-MeOH-Py ²⁺	171.9	1.366	−0.062	−0.079

^a All the averages were performing considering only the four central rings.

^b Average inter-ring dihedral angle N–C–C–N (in degrees).

^c $r_{\alpha,\alpha}$ is the average inter-ring bond distance (in Å).

^d δ_{inter} is the average inter-ring bond alternation parameter (in Å). See Eq. (1).

^e δ_{ring} is the average intra-ring bond alternation parameter (in Å). See Eq. (2).

in average 10° larger for *n*-MeOHPy²⁺ than for *n*-Py²⁺. Thus, the planarity induced on the former oligomers by the double bond character of the inter-ring bonds produces severe steric clashes between the hydroxymethyl groups and the adjacent rings, i.e. conformational strain. Consequently, geometry optimizations of *n*-MeOHPy²⁺ required huge amounts of computer resources, calculations for *n*-MeOHPy²⁺ with $n > 6$ being computationally prohibitive. This feature suggests that the positive doping of these compounds lead to unstable species.

3.2.2. Electronic properties

The variations of ϵ_g and IP with inverse chain length ($1/n$) for *n*-Py²⁺ and *n*-MeOHPy²⁺ are displayed in Fig. 5. As can

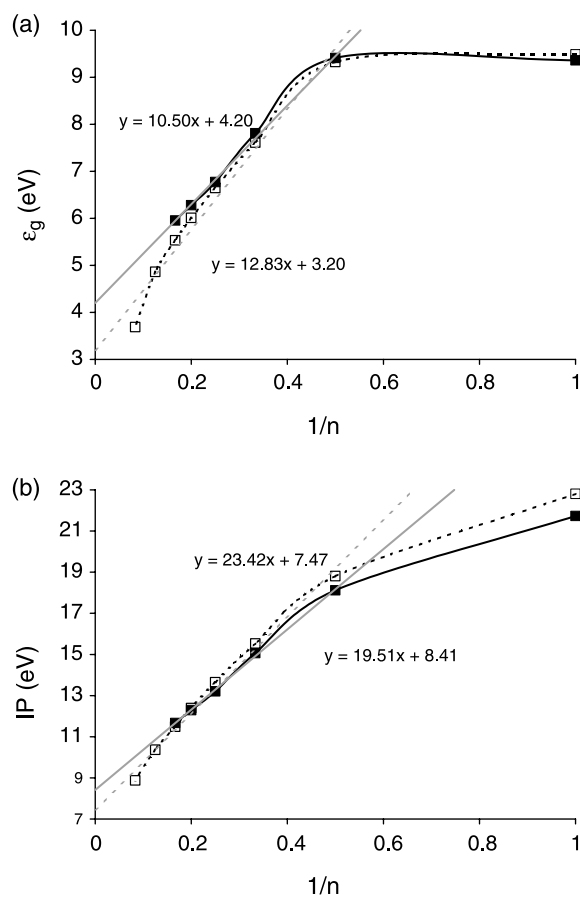


Fig. 5. Evolution of the ϵ_g (a) and IP (b) with inverse chain length ($1/n$) calculated for *n*-MeOHPy²⁺ (black squares, solid lined) and *n*-Py²⁺ (white squares, dashed line) using fully optimized geometries.

be seen the two electronic properties follow a linear behavior for $n \geq 2$. Furthermore, the ε_g calculated for n -Py⁺² is lower than that predicted for n -MeOHPy⁺². Linear regression analyses, excluding the values for $n=1$, were performed to extrapolate the ε_g values for infinite chains of Py⁺² and MeOHPy⁺². Results, which are included in Fig. 5, provided values of 3.20 and 4.20 eV, respectively. It should be noted that the introduction of two positive charges reduces the ε_g of planar poly(Py) and poly(MeOHPy) by about 60 and 42%, respectively. These results are consistent with the molecular geometries described above. Thus, although the two charged systems adopt an all-anti conformation, the inter-ring dihedral angles obtained for n -Py⁺² after geometry optimization are closer to 180° than those achieved for n -MeOHPy⁺². Consequently, the π -conjugation between the rings is more effective in the n -Py⁺² oligomers and the ε_g values are smaller for n -Py⁺² than for n -MeOHPy⁺². However, it should be noted that for $n=1$, where the influence of the planarity cannot appear, the ε_g of 1-MeOHPy⁺² is 0.12 eV smaller than that of 1-Py⁺².

On the other hand, the IP computed for n -Py⁺² is slightly higher than that obtained for n -MeOHPy⁺² when n ranges from 1 to 5, the opposite tendency being detected for larger oligomers. The IP values extrapolated for an infinite chain of poly(Py)⁺² and poly(MeOHPy)⁺² are 7.47 and 8.41 eV, respectively. This considerable difference, 0.94 eV, reflects that N -hydroxyalkyl substitution induces a notable destabilization of the LUMO in the charged polymer.

4. Conclusions

In this work, we have used ab initio quantum chemical calculations to analyze the structural and electronic effects induced by the N -hydroxymethylation of polypyrrole in both undoped and p-doped states. Regarding to the neutral states, both poly(Py) and poly(MeOHPy) exhibit benzenoid structures. If these structures become planar in the solid state, the band gap of poly(MeOHPy) should be lower than that of poly(Py). However, the p-doping process of poly(Py) seems to be slightly more favorable than that of poly(MeOHPy), as indicate their corresponding extrapolated IP values. On the other hand, examination of the positively charged species reveals their characteristic planar quinoid structure. However, the calculations suggest a low stability of the n -MeOHPy⁺² oligomers due to the steric interactions that induce the hydroxymethyl groups. Furthermore, N -hydroxymethyl substitutions on polypyrrole produce a considerable destabilization of the LUMO, in such a way that the band gap extrapolated for positively charged poly(Py) is lower than that of positively charged poly(MeOHPy). This is expected to affect not only

the conductivity and the ability to be n-doped but also the absorption bands and the optical splitting, which are related with optical applications of these materials. Accordingly, the incorporation of N -hydroxymethyl groups alters both the solubility of the polymer in polar environments and specific electronic properties that are essential for technological applications.

Acknowledgements

This work has been supported by MCYT and FEDER with Grant MAT2003-00251. Authors are indebted to the Centre de Supercomputació de Catalunya (CESCA) and the Centre Europeu de Paral·lelisme de Barcelona (CEPBA). COC acknowledges financial support from the Generalitat de Catalunya (DURSI) and the European Social Fund.

References

- [1] Demanze F, Cornil J, Garnier F, Horowitz G, Valat P, Yassar A, et al. *J Phys Chem B* 1997;101:4553.
- [2] Díaz-Quijada GA, Weinberg N, Hodecroft S, Pinto BM. *J Phys Chem A* 2002;106:1266.
- [3] Salzner U. *J Phys Chem B* 2002;106:9214.
- [4] Alemán C, Casanovas J. *J Phys Chem A* 2004;108:1440.
- [5] Gatti C, Frigerio G, Benincori T, Brenna E, Sannicolò F, Zotti G, et al. *Chem Mater* 2000;12:1490.
- [6] Diaz AF, Castillo J, Kanazawa KK, Logan JA. *J Electroanal Chem* 1982; 133:233.
- [7] Diaz AF, Castillo J, Logan JA, Lee W-Y. *J Electroanal Chem* 1981;129: 115.
- [8] Demanze F, Cornil J, Garnier F, Horowitz G, Valat P, Yassar A, et al. *J Phys Chem B* 1997;101:4553.
- [9] Brédas J-L, Street GB, Thémans B, André JM. *J Chem Phys* 1985;83: 1323.
- [10] Casanovas J, Cho LY, Ocampo C, Alemán C. *Synth Met* 2005;151:239.
- [11] Frisch MJ, et al. *Gaussian 98, Revision A.7*. Pittsburgh, PA: Gaussian, Inc.; 1998.
- [12] Hariharan PC, Pople JA. *Chem Phys Lett* 1972;16:217.
- [13] Koopmans T. *Physica* 1934;1:104.
- [14] Alemán C, Armelin E, Iribarren JI, Liesa F, Laso M, Casanovas J. *Synth Met* 2005;149:151.
- [15] Miertus M, Scrocco S, Tomasi J. *Chem Phys* 1981;55:117.
- [16] Hawkins GD, Cramer CJ, Truhlar DG. *J Chem Phys B* 1998;102:3257.
- [17] Jang YH, Goddard III WA, Noyes KT, Sowers LC, Hwang S, Chung DS. *J Phys Chem B* 2003;107:344.
- [18] Iribarren JI, Casanovas J, Zanuy D, Alemán C. *Chem Phys* 2004;302:77.
- [19] Duarte HA, Duani H, De Almeida WB. *Chem Phys Lett* 2003;369:114.
- [20] Kofranek M, Kovar T, Karpfen A, Lischka H. *J Chem Phys* 1992;96:4464.
- [21] Cornil J, Gueli I, Dkhissi A, Sancho-Garcia JC, Hennebicq E, Calbert JP, et al. *J Chem Phys* 2003;118:6615.
- [22] Dkhissi A, Beljonne D, Lazzaroni R, Louwet F, Groenendaal L, Brédas JL. *Int J Quantum Chem* 2003;91:517.
- [23] Alemán C. *Macromol Theory Simul* 1997;6:237.